Title

A Systematic Approach to Corrosion-Powered Sensor Network Design

Authors

Ouellette, Scott
Todd, Michael

Publication Date

2013-09-16

DOI

10.1115/smasis2013-3191

Peer reviewed

Proceedings of the ASME 2013 Conference on Smart Materials, Adaptive Structures and Intelligent Systems
SMASIS2013
September 16-18, 2013, Snowbird, Utah, USA

SMASIS2013-3191

A SYSTEMATIC APPROACH TO CORROSION-POWERED SENSOR NETWORK DESIGN

Scott Ouellette
Department of Structural Engineering
University of California – San Diego
La Jolla, CA, USA

Michael Todd
Department of Structural Engineering
University of California – San Diego
La Jolla, CA, USA

ABSTRACT

Energy harvesting systems for structural health monitoring applications may be described by three stages: ambient energy transduction, electrical power conditioning, and data acquisition and transmission. Recent developments in low-power CMOS devices have allowed for expanded energy harvesting techniques by reducing the total power demand of sensor nodes.

This paper investigates the system-level interaction between a corrosion-based energy harvester and the low-power sensor node to which it is supplying power. An equivalent circuit model of the energy harvester is developed and the matched parameters (source voltage and equivalent series resistance) are used in the design of the power conditioning and wireless transmitter circuitry. Analysis of the power demand from the sensor node is used to determine the optimum data sampling parameters in terms of available supplied power for long-term *in-situ* sensing operations on a marine structure.

INTRODUCTION

Corrosion is a damaging process to the global infrastructure by initiating structural imperfections that ultimately lead to stress concentrations. For decades, engineers have studied methods to control corrosive processes from inflicting damage to critical structural components. One such method that has been used is cathodic protection by means of a sacrificial anode [1]. This method exploits the Galvanic series corrosion process in which two dissimilar metals subjected to a common corrosive electrolyte will create an electrical potential whereby the less noble metal (anode) will be consumed. In terms of corrosion engineering, this method, while proven, is sub-optimal because the consumed anode will eventually need replacement, and thus maintenance costs are inherent to the solution. However, since corrosion is an electrochemical process, there exists a potential to exploit the electrical energy generated to power a sensor network for structural health monitoring applications.

A general energy harvesting paradigm may be parsed into three design stages: energy source, power conditioning, and sensing & communications. It is most commonly the case that the sensing & communications stage is neglected as it tends to fall within the scope of structural health monitoring. However, the process of acquiring measurements, converting the analog signal to digital logic, and transmitting the information requires power; and thus it must remain relevant in the design parameters of an energy harvesting system. This paper attempts to present an integrated approach to the energy harvesting paradigm by accounting for the additional power consumption required during information transmission, and using that information to determine the operational lifetime of the proposed energy harvester.

Energy sources can be classified based by the mechanism in which the transducer operates to generate electrical energy. Each energy source has a unique electrical characteristic that requires careful design of power conditioning circuitry. For example, mechanical (vibration-based) energy harvesting platforms produce an AC power signature, which requires rectification prior to supplying power to a microcontroller (MCU).

Power conditioning circuitry often operates at low-voltage or even sub-CMOS voltage levels. In most cases, a DC-DC converter is needed to alter (buck or boost) and regulate the supply voltage delivered to an MCU. This is a critical step in the design of sensor networks, as the amount of power consumed by the conditioning circuitry must be minimized in order to prolong the operational lifetime of an autonomous sensing system.

This paper first analyzes the electrochemical process of corrosion to exploit the available energy to potentially power a wireless sensor network. A Galvanic series battery is developed from the corrosion principles, and experimental tests are

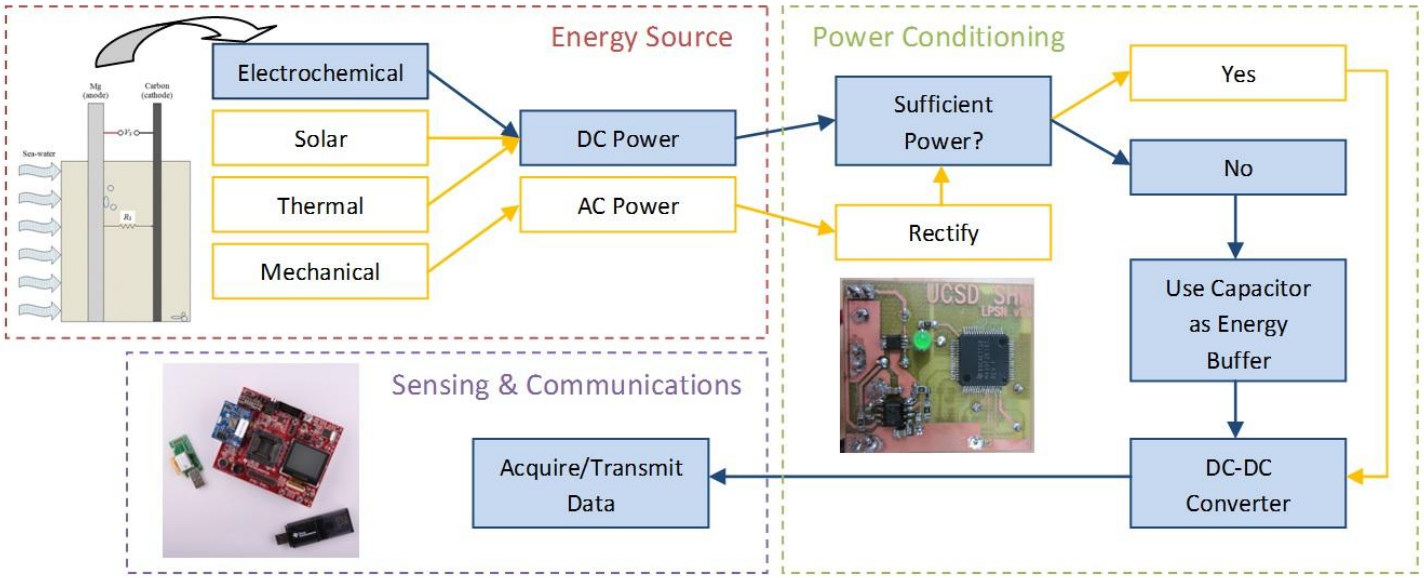

Figure 1. General description of the energy harvesting paradigm for wireless structural health monitoring applications. Included images comprise the components of the proposed autonomous wireless sensor node system.

conducted to determine the output power characteristics. Measured parameters are implemented in the equivalent circuit model and used for the design of a low-power DC-DC converter needed for providing regulated CMOS voltage to a low-power microprocessor and wireless transmitter. Power consumption of the sensor node is investigated in detail and is used to determine the necessary anode mass to sustain the total power demand for long-term monitoring operations.

ENERGY SOURCE

Corrosion of concrete reinforcing steel rebar is a primary failure mode of marine structures (e.g. bridges, piers, ports), and is the motivating factor in the development of the corrosion-enabled energy harvester. In order to understand the choice in using Galvanic series corrosion as an energy harvesting approach, it is important to first understand the mechanism in which corrosion affects reinforcing steel rebar inside of concrete.

The corrosion of steel in concrete occurs most commonly in seawater due to the increased amounts of chloride in the form of salt. The corrosion process itself is defined by the removal of iron atoms from the steel surface. This process only occurs at locations on the steel surface that have direct contact with the seawater, as concrete is a porous material. Since corrosion is an electrochemical process, the transfer of electrons from anode to cathode is required to maintain charge neutrality. The reaction at the cathode (gaining electrons) occurs simultaneously with the anodic reaction, and the pair of reactions is referred to as an oxidation-reduction (redox) reaction. For a single bar of steel, the anodic and cathodic initiation sites are determined by intrinsic material imperfections in concert with the concrete interface, and the voltage generated in the reaction is correlated to the atomic properties of steel, also known as the electromotive force (emf).

There are several reasons why using just the corroding steel as the energy generator for a sensor network is undesirable, not the least of which being the active promotion of corrosion for a load bearing structural element. Therefore, for several other reasons not listed, this paper will present the design of a Galvanic series corrosion energy harvester, appropriately referred to as a cement battery.

Galvanic Series Battery

As stated earlier, the Galvanic series battery approach requires two dissimilar metals to either corrode in the same electrolyte, or to share a common electrical contact. The design implemented in this initiative (as seen in Figure 1) incorporates a cement cylinder as a porous barrier between the two metals, and immerses the system in a seawater bath [2]. Direct electrical contact is achieved when the battery is connected to a resistive load. The metals selected for this study were Magnesium (Mg) and Carbon/graphite. This choice was based on the high relative Galvanic electrical potential, as well as their inexpensive cost. The redox reaction that describes the electron transfer of the battery is shown below in equation (1) in terms of the two half reactions:

$$\begin{aligned} Mg &\rightarrow Mg^{2+} + 2e^- \\ O_2 + 2H_2O + 4e^- &\rightarrow 4OH^- \end{aligned} \quad (1)$$

It is assumed there are no carbon ions in the electrolyte to be reduced to carbon atoms for a cathode reaction. Since the electrolyte (seawater) pH generally ranges between basic and neutral depending on local environmental conditions, oxygen

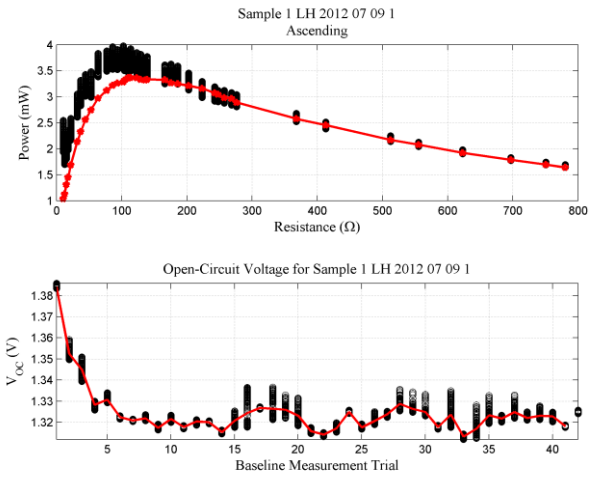

Figure 2. Cement battery output power characteristic curve for a resistive load sweep (top) and the measured open-circuit voltage for the battery between each resistive load measurement (bottom). Overlaid in red is the Thévenin equivalent power curve with the input voltage being the measured open-circuit voltage.

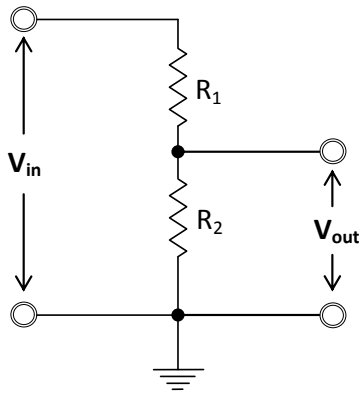

Figure 3. Voltage divider model representing cement battery energy harvester connected to a resistive load.

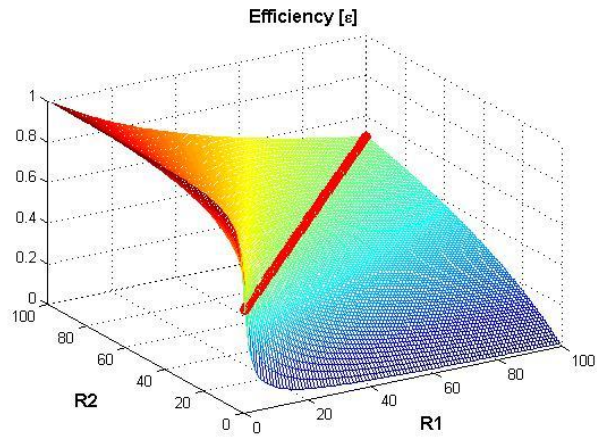

Figure 4. Power transfer efficiency for a voltage divider circuit for a range of values for both resistors, with the matched impedance efficiency overlaid in red.

and water molecules will react to form hydroxyl ions. By representing the redox reaction as two half-reactions, it can be noted that charge neutrality will require two magnesium atoms to be oxidized for each reduced oxygen molecule.

A unique secondary reaction occurs in this design as a result of the compositional heterogeneity inherent in the cement structure. Since the metallic surface of the anode is not uniformly exposed to the seawater, there exists a local corrosion initiation site at the anode-pore interface. This results in a pitting reaction as described by equation (2) below:

$$Mg(Cl)_2 + 2H_2O \rightarrow Mg(OH)_2 + 2HCl \qquad (2)$$

The highly acidic hydrochloric acid (HCl) byproduct of this reaction causes an increase in the corrosion rate of the anode (i.e. self-discharge of the battery). This process would become autocatalytic if not for the reduced amount of oxygen present due to the cement barrier acting as a diffusion rate limiter.

Equivalent Circuit Model

It is often instructive to develop an equivalent circuit model for later use towards the design and development of the power conditioning circuitry. For battery-type energy harvesting devices, a good starting model is Thévenin's equivalent circuit. This model parameterizes a two terminal system into an ideal voltage source with a series resistor. A cursory review of corrosion literature suggests a slightly more exotic circuit model for oxidizing metals in concrete; however, the leading-order behavior for ohmic loads is accurately modeled by the Thévenin equivalent, and thus works well for this study.

Determining the equivalent series resistance for the cement seawater battery is accomplished by a resistive load sweep in which the peak measured power occurs at a matched load. For the purposes of this study, the resistive load sweeps were performed bi-directionally to test the source linearity. Based on the experimental data shown in Figure. 2, the source resistance can be estimated to be 150Ω. The experimental setup, however, leads itself to a relatively high parasitic resistance due to the number of clip-connections and the length of wire used for the measurement probes.

Several energy harvesting papers have focused on developing the power electronics with an equivalent resistance to the source resistance, a process referred to as impedance matching [3], [4], [5]. For a simple ohmic load, the peak power transfer for a Thévenin-type source occurs at matched impedance. A circuit diagram of this scenario is shown in Figure. 3. Using Ohm's law to solve for V_{out} gives:

$$V_{out} = \frac{V_{in}R_2}{R_1 + R_2} \qquad (3)$$

For matched impedance, $R_1 = R_2$ and thus:

$$(V_{out})_{max} = \frac{V_{in}}{2} \quad (4)$$

and:

$$(P_{out})_{max} = \frac{(V_{out}^2)_{max}}{R_2} = \frac{V_{in}^2}{4R_2} \quad (5)$$

As seen in equation (4), the maximum output power at matched impedance is scaled by the load resistance (R_2). Therefore, reducing the internal resistance of the power source will ultimately increase the output power.

However, when considering the efficiency of power transfer from source to load, operating at matched impedance is sub-optimal with respect to the power source. In essence, for a finite power supply (e.g. a battery), connecting to a matched impedance load will draw the maximum current. In the case of the cement battery, this situation will result in an increased corrosion rate of the anode being consumed, thus reducing the operational lifetime of the sensor node.

Defining the power transfer efficiency as the ratio of output power to input power, it can be shown that the efficiency of a matched impedance circuit is only 50%.

$$\varepsilon = \frac{P_{out}}{P_{in}} = \frac{V_{out}I_{out}}{V_{in}I_{in}} \quad (6)$$

Using Ohm's law to solve for the current expressions results in:

$$\varepsilon = \left(\frac{V_{out}}{V_{in}}\right)^2 \left(\frac{R_1}{R_2} + 1\right) \quad (7)$$

Substituting V_{out} from equation (3) yields an expression for efficiency purely in terms of resistance:

$$\varepsilon = \frac{R_2}{R_1 + R_2} \quad (8)$$

Analysis of equation (8) shows that power transfer efficiency increases greatly for the condition $R_2 >> R_1$, as seen in Figure. 4. Thus for an energy harvesting system with finite supply, a sensor node with a large effective resistance is optimal. This criterion does, however, require special consideration when designing the power conditioning electronics because of the reduced current flow through the load. The following section will present one possible solution to this matter by way of an energy buffer and load isolation.

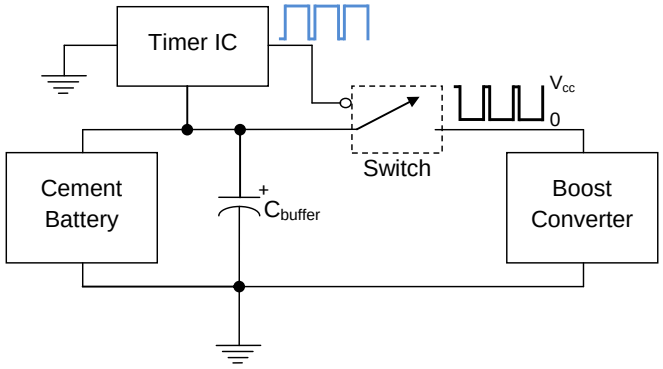

Figure 5. Schematic diagram of the low on-resistance analog switch and energy buffering capacitor

POWER CONDITIONING

The intermediate step of the energy harvesting paradigm consists of conditioning the output electrical signal from the energy harvester into a useful DC source for sensing and communication electronics. For the purposes of this study, this section deals with the implementation of a low-power DC-DC boost converter and a unique energy buffer isolation architecture to more efficiently transfer power to the electrical load. Careful consideration to the power demands of each stage of the sensor node is applied to the design in order to prolong the potential operational lifetime of the autonomous sensor node platform.

Energy Buffer & Analog Switch

Analysis of the output power characteristics of the cement battery prohibits the direct application of a DC-DC boost converter due to the current demand by most commercially available boost converter ICs. Therefore, it is necessary to use an energy buffer (typically a super-capacitor) to function as the power supply for the boost converter, sensor node, and wireless transmitter. By implementing a low on-resistance analog switch in conjunction with a 100mF super-capacitor (as seen in Figure. 4), the cement battery can store energy for a defined time interval, and then rapidly discharge the energy for sensing and communications.

The analog switch (SN74AUC2G53, Texas Instruments) is a low-voltage single-pole, double throw (SPDT) switch that isolates the buffer capacitor from the boost converter, MCU, and transmitter. It is important that this switch has a low on-resistance in order to avoid losses in power transfer to the boost converter. The switch is controlled by a low-voltage, low-power timer IC (TLC 551, Texas Instruments) set to generate a very low duty cycle PWM signal. It is important to note that the analog switch and timer IC must be able to operate with a low supply voltage (~1V) and have a minimal current consumption. Between the analog switch and timer IC, there is only 303µW of power consumption for operation, with the switch having an additional 1µA leakage current.

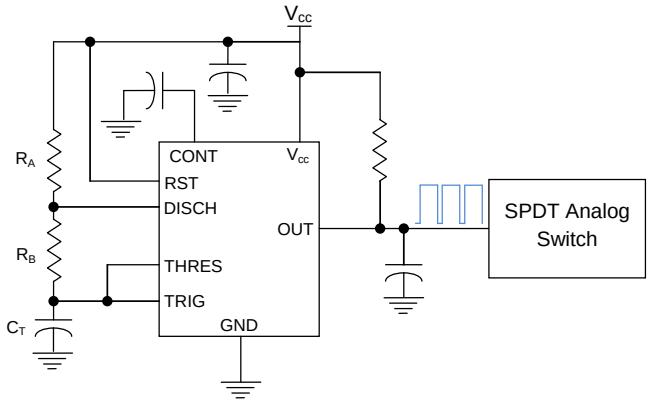

Figure 6. Schematic diagram of the low-power timer IC.

The main concept at work with this use of an energy buffer stems from the desire to have the sensor node operate from a single cement battery supply. Using a capacitor to provide power enables a circuit to drive high load demands. This is because the power delivered by a capacitor is a function of its inherent capacitance, the charge voltage, and, most importantly, the rate at which it discharges its voltage, as shown in equation (9).

$$P_{capacitor} = CV\frac{dV}{dt} \tag{9}$$

Taking advantage of this fact, this design can provide enough power for all the sensing and communication needs by simply tailoring the PWM control signal from the timer IC.

Timer IC

The timing control signal circuit is essential to the overall sensor node operation, as it sets the functional period of the device. The charge/discharge time is set by the resistor pair (R_A, R_B), and is scaled by the threshold capacitor (C_T) as seen in Figure. 5. The equations that approximately describe the output PWM duty cycle and frequency are shown below [6]:

$$\begin{Bmatrix} t_{on} \\ t_{off} \end{Bmatrix} \approx C_t ln2 \begin{bmatrix} 1 & 1 \\ 0 & 1 \end{bmatrix} \begin{Bmatrix} R_A \\ R_B \end{Bmatrix} \tag{10}$$

Due to the internal architecture of this specific device, it is extremely difficult to generate a duty cycle lower than 50%, the only method being to drive R_A below the internal device resistance. Given the power demands of the sensor node, and the total output power of the cement battery, it is imperative that the charge/discharge cycle of the buffer capacitor must be less than 50% for the energy transfer to be optimal. Therefore, the only option is to set the circuit parameters to generate a very high duty cycle (~99%) and to invert the signal on the control pin of the analog switch. This can be done two ways: 1) implement a simple inverter circuit using an OpAmp, or 2) exploit the internal logic within the SPDT analog switch. For ease of implementation, option 2 was chosen by connecting the output of the switch to the logic scenario when the control input and reference voltage are low (GND). For the purposes of this study, the desired on-time/off-time PWM signal was chosen such that the buffer capacitor would drain for 20ms for every 1-minute period. A detailed power analysis of the entire sensor node, accounting for the MCU and transmitter, will demonstrate a more optimal duty cycle.

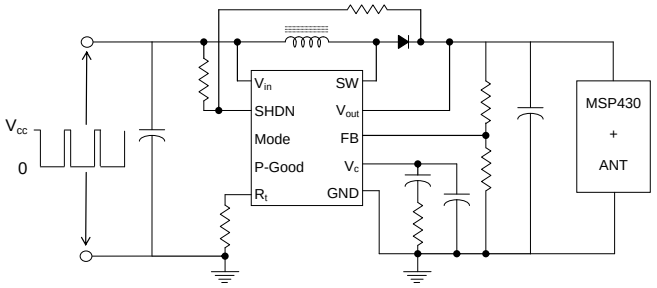

Figure 7. Schematic of boost converter design.

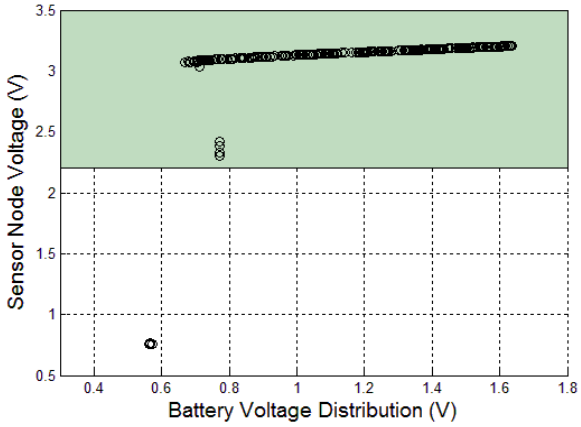

Figure 8. Output voltage distribution of low-power boost converter with MCU connected and operating.

Boost Converter

The output voltage signal from the discharging capacitor is a low duty cycle square wave. The boost converter used in this initiative features a low-voltage micro-power step-up switching regulator IC (LTC3402, Linear Technology). This IC is feedback regulated to provide an adaptive switching frequency which holds the output voltage of the boost converter constant. The component values were chosen to provide a stable 3V supply to the MCU and transmitter.

Due to the variability in output voltage of the cement battery, Monte Carlo simulations were performed using LTSpice IV (Linear Technology) on the component value variability, as well as input voltage variability to verify robust boost converter operation and a stable output voltage. The circuit model consisted of the 100mF buffer capacitor

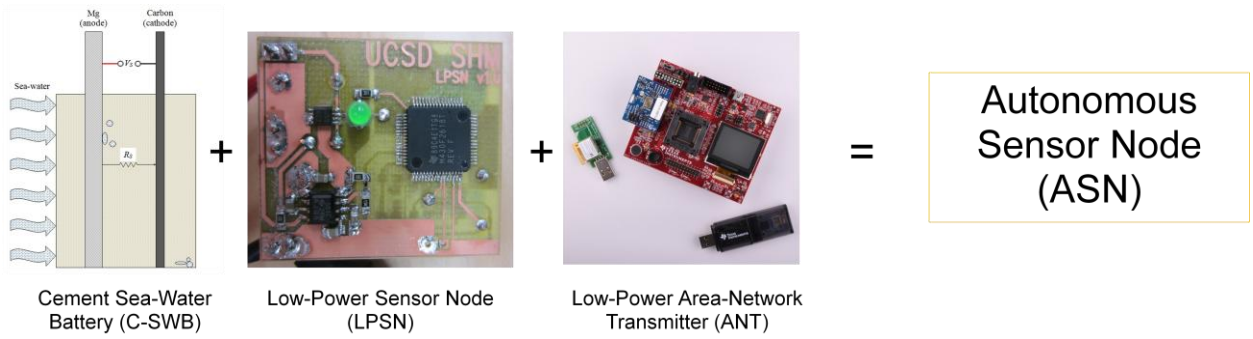

Figure 9. Components of the proposed autonomous sensor node system.

supplying power to the boost converter in 20ms intervals across an ideal switch controlled by a set PWM voltage signal. The charge voltage on the supply (buffer) capacitor varied from 0.5-1.8V, and the MCU was modeled as a piecewise linear varistor to account for the power consumption between two programmed states of operation, active mode (AM) and low-power mode (LPM0).

The results of this parametric study suggested the boost converter would be capable of producing an output voltage of 3V ± 100mV over an input voltage range of 0.6-1.8V. The cutoff voltage of the boost converter is mainly a result of the rectifying output diode requiring 600mV to conduct. A prototype printed circuit board (PCB) of the energy buffer and boost converter design was fabricated and tested in the lab. A lab-bench power supply with an equivalent series resistance was used to emulate the cement battery power as designed, and the output voltage was probed to validate the simulation results.

SENSING & COMMUNICATIONS

The final step in the development of an autonomous wireless sensing platform concerns the acquisition and management of measurement information. From a development standpoint, this stage offers multiple options in terms of sensing type (e.g. strain, temperature, acceleration, etc.) and network configuration. Furthermore, there exists a plethora of manufacturers and product solutions to choose from. This section describes the decision rationale for the choice of MCU and wireless transmitter. To date, a prototype sensor node has be fabricated and tested without the addition of the wireless transmitter system [7]. The initial results are promising in terms of the sensor node being capable of operating from the output power provided by the cement battery.

Texas Instruments MSP430 and ANT

The TI MSP430 is an ultra-low power family of mixed-signal microprocessors for portable applications. The specific device used in this study features a wide supply voltage range (2.2-3.6V) and low power consumption in active mode. In terms of input/output (I/O) capability, this device has six channels, a 12-bit ADC, and 116kB onboard flash memory. Most importantly, the internal architecture of the MSP430 family has five programmable power modes for extending battery life. In active mode, operating at a 1MHz clock frequency, the device consumes at most 560μA (with a 3V supply).

The wireless transmitter/receiver chosen for this study is the ANT CC2571 (Texas Instruments) short-range transceiver network. This product was chosen because of its simple interface with the MSP430 devices. Furthermore, it also features very low power consumption, a user-friendly software programming interface, and a very flexible master/slave network protocol. This particular model features up to 8 transmission channels, and upwards of 200Hz broadcast frequency.

Together, the MSP430 and ANT CC2571 complete the sensing and communications needs for the sensor network. When combined with the cement battery and power conditioning circuitry, the sensing system is entirely autonomous (see Figure. 8).

POWER ANALYSIS & OPERATIONAL LIFETIME

As mentioned earlier, the timing of the analog switch was pre-determined based on the decision to allow for the buffer capacitor to fully charge prior to taking a measurement and transmitting the data. This timing sequence turns out to be a bit conservative in terms of the optimal charge/discharge rate of the buffer capacitor. This section investigates the power consumption of the sensor node and uses that information to determine the peak measurement rate for the autonomous wireless sensor node operating at max power consumption. The power consumption analysis is then used to determine the necessary anode volume for a long-term sensing operation.

Calculation of Total Load

The total load (mW) is calculated as the sum of all the active power consuming elements on the sensor node (resistors, capacitors, and inductors are neglected due to their small power consumption). The elements that comprise the list are: 1) the analog switch, 2) the timer IC, 3) the boost converter, 4) the MCU, and 5) the transmitter. Reviewing the datasheets for these devices yields the power consumption table (see Table 1 below).

Table 1 Sensor Node Power Consumption

Device	Supply Voltage	Supply Current	Power Consumption
SN74AUC2G53	1.3V	10μA	13μW
TLC 551	1.3V	225μA	0.29mW
LTC 3402	1.3V	800μA	1.04mW
MSP430	3V	560μA	1.68mW
CC2571	3V	3430μA	103mW

The total power consumption of the sensor node calculates to approximately 106 mW. A cursory observation of the table shows that the majority of power is applied to transmitting the data. The value for the transmitting current was obtained from the assumption that the transmitter would be operating at 4-dBm output power.

Converter Efficiency and Capacitor Charge Dynamics

When evaluating the total power consumption demand of the circuit, it is also important to consider the efficiency of the boost converter operation. Based on the measured performance efficiency as a function of output current, as provided by the manufacturer, the converter efficiency is assumed to be 90%. Therefore, the amount of power required for sensor node operation must account for the 10% loss during voltage conversion. The total required input power is then obtained by dividing the sensor node power consumption by the converter efficiency.

$$P_{in} = \frac{P_{sensor\_node}}{\varepsilon_{boost}} \tag{11}$$

Based on this condition, the amount of input power needed to operate the sensor node is approximately 118mW. Dividing the input power by the supply voltage (1.3V) yields a current consumption of approximately 91mA. Assuming the input current comes from the buffer capacitor, and further assuming the drain current from the capacitor is constant, then the total time for the buffer capacitor to discharge from 1.3V is calculated from equation (12) below, where i_{out} is defined as the output current from the capacitor, which is the current demand of the sensor node.

$$dt_{out} = \frac{CdV}{i_{out}} \tag{12}$$

For a buffer capacitor with 100mF capacitance, the total discharge time is calculated as 1.43s. That is roughly seven-times the length of operation time than the pre-determined duty cycle of the analog switch gate. However, this does not account for current spikes on device startup, so the total discharge time most likely is slightly less than estimated.

Determining the total charge time for the capacitor requires the knowledge of the source resistance of the cement battery. This was experimentally measured as approximately 150Ω. A capacitor charges exponentially under a constant applied voltage defined by:

$$V_{charge} = V_{in}\left(1 - e^{-t_{charge}/RC}\right) \tag{13}$$

Solving equation (13) for the charge time (t) results in a logarithmic charge time defined as:

$$t_{charge} = -R_S C \ln\left(1 - V_{charge}/V_{in}\right) \tag{14}$$

Assuming a charge voltage of 1.3V, and an input voltage of 1.4V (this can vary depending on Galvanic potential between the anode and cathode), the total charge time for the buffer capacitor is calculated as approximately 40s. Applying this charge time to equation (12) will determine the output current of the cement battery, which is calculated at 3.25mA.

The conditions reported in this analysis represent the peak operational duty cycle for the autonomous sensor node operating at max power consumption. The effect of this scenario will be applied to the corrosion dynamics of the cement battery to determine the necessary anode volume (assuming a cylindrical shape) for an operational period of 50 years – similar to that of a large-scale marine structure.

Cement Battery Operational Lifetime

Based on the power demand of the sensor node, the necessary corrosion current required for charging the buffer capacitor was determined. The corrosion current is equivalent to the rate of corrosion of the anode, thus allowing for the application of Faraday's equation of general chemistry [8]:

$$w = \frac{ItM}{nF} \tag{15}$$

where w is the weight of the corroding material [grams], I is the current flow [Amperes], M is the atomic mass for the metal [gram mol^{-1}], n is the number of electrons transferred in the reaction [n = 2 for Mg], and F is Faraday's constant [A s mol^{-1}]. Dividing both sides of equation (15) by the density (ρ) yields an expression for the volume of anode as a function of the current flow and time.

Adjusting the current flow I for the duty cycle for charging the buffer capacitor, and assuming the operational time for the sensor node is 50 years; the necessary anode volume is calculated at approximately 359cm^3, which is approximately 625 grams. Bulk magnesium is currently priced at $0.29 per 100 grams. Thus, for a sacrificial anode of magnesium operating for 50 years at peak power consumption for, the total cost will be approximately $1.82, assuming the entire anodic material is consumed.

CONCLUSIONS

This paper describes an integrated system-level energy harvester design enabled by the process of corrosion. A general energy harvesting paradigm is presented, and each stage is presented in detail with regards to the project. A description of the electrochemical process that governs the energy harvester (cement battery) is provided. Recommendations for the effective resistance of the sensor node are given for improved power transfer efficiency based on the assumed equivalent circuit characteristics of the battery.

Next, the power conditioning electronics is presented in the order in which they manage the transfer of power from the energy harvester to the sensing and communications hardware. Lastly, a detailed power analysis of the entire sensor node is provided, and an example design scenario is presented in order to estimate the necessary anode volume for a long term operational study.

ACKNOWLEDGMENTS

This initiative was supported by a National Science Foundation Graduate Research Fellowship. Special thanks to Phil Zerofski at Scripps Institution of Oceanography (SIO) for providing access to laboratory space for conducting experiments on the cement battery energy harvester. The authors would also like to thank Richard Do, Cory Youngdale, and Joao Cheong for co-executing experiments at SIO.

REFERENCES

[1] D. A. Jones, *Principles and Prevention of Corrosion*, 2nd ed. Prentice Hall, 1995.

[2] S. A. Ouellette, D. D. L. Mascarenas, and M. D. Todd, “Corrosion-enabled powering approach for structural health monitoring sensor networks,” pp. 728821–728821, Mar. 2009.

[3] H. Kim, S. Priya, H. Stephanou, and K. Uchino, “Consideration of impedance matching techniques for efficient piezoelectric energy harvesting,” *Ultrason. Ferroelectr. Freq. Control Ieee Trans.*, vol. 54, no. 9, pp. 1851–1859, 2007.

[4] L. R. Clare and S. G. Burrow, “Power conditioning for energy harvesting,” in *Proc SPIE*, 2008, vol. 6928, p. 69280A.

[5] N. A. Kong, D. S. Ha, A. Erturk, and D. J. Inman, “Resistive impedance matching circuit for piezoelectric energy harvesting,” *J. Intell. Mater. Syst. Struct.*, vol. 21, no. 13, pp. 1293–1302, 2010.

[6] Texas Instruments, “TLC 551 LinCMOS Timers.” Sep-1997. http://www.ti.com/lit/ds/slfs044b/slfs044b.pdf

[7] S. A. Ouellette and M. D. Todd, “Uncertainty quantification of a corrosion-enabled energy harvester for low-power sensing applications,” 2013, p. 86921G–86921G–8.

[8] W. F. Smith and J. Hashemi, *Foundations of Materials Science and Engineering*, 4th ed. McGraw-Hill, 2005.